Tecnun
Universidad
de Navarra

Studies: Biomedical engineering
Subject: Biomechanics & Biorobotics

Practical work: human motion reconstruction

2024-2025

Group 10

Alessandro Giuseppe Milazzo
Paolo Pagliaro

1. INTRODUCTION AND OBJECTIVES

Motion capture systems are used globally in many different fields, measuring human body segments and tracking their movement, in fact, has become very important in different applications; from film special effects to health care, sport performance analysis and human machine interaction are only some examples [https://doi.org/10.1108/SR-10-2018-0270]. Motion capture is a technology used to record and analyse the movement of a subject in the three-dimensional space. Optical, inertial, magnetic or mechanical sensors are used to track position, velocity and acceleration of points on the moving body.

A wide portion of experiments and studies is based on the track and acquisition of movements with multiple synchronized cameras. [1] In the present work a camera-based OptiTrack motion capture system has been used; the use of OptiTrack systems is increasing year after year, as demonstrated by the rising number of scientific publications relying on it.

To carry out these processes, specific tools called “markers” are used: they are small objects fixed on the body of interest, which allow to track the movement of it; they can be active or passive. Active markers are led able to emit IR light which gets detected by the cameras of the system; passive markers are small spheres or disks covered by reflective material which simply reflect IR light emitted by a ring of leds present in the cameras. In this work, a system based on passive markers has been used.

Cameras involved in Mocap studies based on passive markers have specific features; they’re composed by leds emitting light in IR spectrum and by an objective through which light that gets reflected by markers is detected. In the system used, cameras’ leds are arranged in a ring-shape with the objective in the central part of the ring.

Usually, markers are placed at specific points depending on the goal of the experiment. In some applications, for example, they can be positioned on specific anatomical landmarks, typically easy to identify and not subject to relative motion between the skin and underlying structures.

As mentioned above, markers’ movement is detected and tracked by cameras, data are collected and then processed by the system; using the two-dimensional view from multiple cameras, the system is able to reconstruct the three-dimensional position of the markers. Each cameras tracks and records the position of markers in the two-dimensional space, but overlapping and processing data collected form more cameras allow to reconstruct markers’ position in the three-dimensional space. To reconstruct the 3D position of a marker, the system needs at least two cameras which see the marker of interest, that is why it is important to have systems equipped with more cameras.

These kinds of systems can be very accurate and allow a very precise reconstruction of trajectories and movements enabling quantitative analysis. The system used in the present work is featured by a resolution of 1 mm.

Defining the capture volume is also a crucial step, it depends on the space required to perform the task and, naturally, on the dimensions of the laboratory. A larger capture volume requires more cameras and greater distances between them; on the other hand, a small

capture volume can limit number of movements that can be analysed (some movements require larger spaces, gait analysis for example requires the physical space to perform few steps).

Motion capture technology has a wide variety of applications, in particular in the biomechanics field. In gait analysis is possible to identify abnormalities in walking patterns, useful both for clinical diagnosis and for treatments; in sport fields these systems are used to optimize athletic performances and to prevent injuries by studying high degree-of-risk movements; in rehabilitation it's possible to monitor progresses after injuries or surgeries; it's also possible to evaluate and asses the impact of orthopedic devices on patient to optimize treatment outcomes; postural analysis and ergonomics are other two linked fields where mocap can be useful, in particular in the identification of postural stability, compensatory mechanisms and evaluation of the interaction between human and machines.

The goal of this work is to better understand, through a real experiment, how it is possible to reconstruct and analyse human motion with a camera-based motion capture system. Specifically, the objectives are:

- To capture 2 different right leg movement using the Optitrack capture system
- To estimate the parameters of the right leg model
- To define the model using natural coordinates
- To reconstruct the motions
- To analyse reconstructed motions

2. MOTION CAPTURE

2.1. Materials

The Optitrack motion capture system used for the work consisted of 11 cameras strategically positioned in the room. Eight cameras were placed in the four corners of the room (four at the top and four at the bottom), while the remaining three were arranged as follows: two on the right side (one at the top and one at the bottom) and one on the left side, positioned at the top.

The work began with a calibration, an essential phase to ensure the quality of the acquired data. During calibration, the system calculates the position and orientation of each camera and the amount of distortion in the captured images to build a 3D capture volume in the software used. This is done by observing 2D images from multiple synchronized cameras and associating the position of known calibration markers from each camera through triangulation.
It is important to note that if any changes are made to the camera setup or if environmental conditions change, the system must be recalibrated to maintain accuracy.

[2] Calibration phases:

- Preparation of the capture volume: optimization of the space for the motion capture system. The cameras must be positioned and configured appropriately to ensure complete coverage of the capture volume. Each camera must be securely mounted to remain stationary during data acquisition.
- Masking of reflections: before calibration, all foreign reflections or unnecessary markers must be eliminated or covered, to prevent overlaps with the markers relevant for the motion capture. If this is not possible, reflections detected can be masked directly in the software used.
- Sample collection through wanding: wanding is the main phase of calibration. A calibration wand with preset markers is used, shaken repeatedly throughout the volume. This process allows the cameras to detect the markers and collect sample data points, enabling the software to calculate the position and orientation of each camera in 3D space.
- Definition of the ground plane: to complete the calibration, the ground plane must be defined using a custom calibration square, consisting of three markers arranged in a right angle, with one arm longer than the other. The global origin is then set by applying a vertical offset, which represents the distance between the center of the markers on the calibration square and the actual ground.

2.2. Methods

The next phase of this work involved the placement of the markers. Nine markers were positioned as specified in Table 1, maintaining a distance of more than 5 cm between each. Ensuring a distance greater than 5 cm between markers enhances measurement accuracy

by preventing overlaps or interferences that could compromise the precision of movement estimates and joint parameter calculations.

These markers are used for three main purposes:

- Defining the local coordinate system (LCS) of each segment.
- Estimating joint parameters.
- Reconstructing the movements

Segment	Description	Optitrack name (suggestion)
Thigh	Marker on landmark LFE	LFE
	Marker on landmark MFE	MFE
	Marker on the right thigh	RT
Shank	Marker on the right shank	RS
	Marker on landmark LM	LM
	Marker on landmark MM	MM
Foot	Marker on the foot	F1
	Marker on the foot	F2
	Marker on the foot	F3

Table 1:

At this stage, the static posture was recorded, which was later used in the second phase to estimate the model parameters. In this study, the static posture of the right leg was captured with the knee and ankle in a neutral position.

Subsequently, the movements of knee flexion and extension were recorded, starting and ending with the knee in the neutral position. Then, the movements of dorsiflexion and plantarflexion of the ankle were recorded, starting from maximum plantarflexion and proceeding to maximum dorsiflexion. During this phase, the thigh was stabilized with both hands to minimize unwanted movements.

During the motion capture phase not many problems were encountered. The only two aspects that required more time was masking unwanted light sources and the initial calibration of the cameras, due to the limited space in the laboratory.

3. ESTIMATION OF MODEL PARAMETERS

3.1. Definition of joint centers and LCS of each segment

This part of the work started with the calculations to estimate of all the joint's centers needed for the development of the leg model, in particular the Hip-Joint-Center, the Knee-Joint-center and the Ankle-Joint-Center; parameters were calculated according to Table 1.

Knee Joint Center (KJC)

The KJC was computed as the midpoint between the lateral and medial femoral epicondyles:

$$KJC = \frac{LFE + MFE}{2}$$

Ankle Joint Center (AJC)

The AJC was computed as the midpoint between the lateral and medial malleoli:

$$AJC = \frac{LM + MM}{2}$$

Hip Joint Center (AJC)

As the hip has not been considered in the model, HJC was estimated using the subject-specific distance from KJC: in static posture, the distance between KJC and HJC was measured in the global vertical direction, using a tape measure.

Joint	Type	Method
Hip	Not in model	**Joint centre (HJC)**: in the static posture, start at KJC, then in the global vertical direction add the length between KJC and HJC. This length must be measured on the subject.
Knee	Revolute	**Joint centre (KJC)**: midpoint of LFE and MFE. **Joint axis 1 (flexion/extension):** coincident with **Zt = Zs**.
Ankle	Universal	**Joint centre (AJC)**: midpoint of LM and MM. **Joint axis 1 (dorsiflexion/plantarextension):** coincident with **Zs**. **Joint axis 2 (inversion/eversion):** coincident with **Xf**.

Table 2: Joint parameter definitions

After having computed joint's centers, the local coordinates systems (LCS) of the considered body's segments (thigh, shank and foot) were calculated, according to Table 2.

LCS of the Thigh

Yt is defined as the unit vector from KJC to HJC, pointing proximally:

$$\boldsymbol{Yt} = \frac{\boldsymbol{KJC\ HJC}}{\left|\left|\boldsymbol{KJC\ HJC}\right|\right|} = \frac{\boldsymbol{HJC - KJC}}{||\boldsymbol{HJC - KJC}||}$$

Xt is defined as the unit vector perpendicular to the plane containing HJC, LFE, MFE and pointing forward. To calculate the aforementioned unit vector, an auxiliary unit vector a was computed:

$$\boldsymbol{a} = \frac{\boldsymbol{MFE\ LFE}}{\left|\left|\boldsymbol{MFE\ LFE}\right|\right|} = \frac{\boldsymbol{LFE - MFE}}{\left|\left|\boldsymbol{LFE - MFE}\right|\right|}$$

Finally, Xt was calculated through the vector product between Yt and a:

$$\boldsymbol{Xt} = \boldsymbol{Yt} \times \boldsymbol{a}$$

Zt, is computed through the vector product of Xt and Yt:

$$\boldsymbol{Zt} = \boldsymbol{Xt} \times \boldsymbol{Yt}$$

The origin of the LCS is coincident with KJC. The calculate LCS is showed in fig.1.

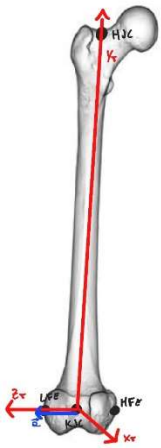

Figure 1: schematic drawing of thigh's LCS

LCS of the Shank

Ys is defined as the unit vector connecting AJC and KJC, pointing proximally:

$$\boldsymbol{Ys} = \frac{\boldsymbol{AJC\ KJC}}{\left|\left|\boldsymbol{AJCKJC}\right|\right|} = \frac{\boldsymbol{KJC - AJC}}{\left|\left|\boldsymbol{KJC - AJC}\right|\right|}$$

Xs is defined as the unit vector perpendicular to the plane containing KJC, LM, MM and pointing forward. To calculate Xs the auxiliary vector a is used again:

$$\boldsymbol{Xs} = \boldsymbol{Ys} \times \boldsymbol{a}$$

Zs is calculated through the vector product between Xs and Ys:

$$\boldsymbol{Zs} = \boldsymbol{Xs} \times \boldsymbol{Ys}$$

The origin of the LCS is coincident with AJC. The calculate LCS is showed in fig. 2.

Figure 2: schematic drawing of shank's LCS

LCS of the Foot

Xf is defined as the unit vector coincident with Xs in static posture.

$$\boldsymbol{Xf} = \boldsymbol{Xs}$$

Yf is defined as the unit vector coincident with Xs in static posture.

$$\boldsymbol{Yf} = \boldsymbol{Ys}$$

Zf is defined as the unit vector coincident with Xs in static posture.

$$\boldsymbol{Zf} = \boldsymbol{Zs}$$

The origin of the LCS is coincident with AJC. The calculate LCS is showed in fig. 3.

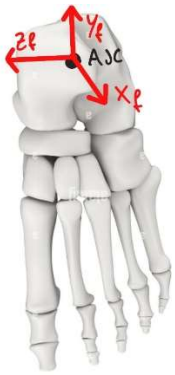

Figure 3: schematic drawing of foot's LCS

Thanks to these calculations, the rotation matrices, composed by unit vectors of the LCSs systems, were calculated:

$$\boldsymbol{Rt} = [\boldsymbol{Xt}, \boldsymbol{Yt}, \boldsymbol{Zt}]$$

$$\boldsymbol{Rs} = [\boldsymbol{Xs}, \boldsymbol{Ys}, \boldsymbol{Zs}]$$

$$\boldsymbol{Rf} = [\boldsymbol{Xf}, \boldsymbol{Yf}, \boldsymbol{Zf}]$$

-01018	0	-0,9889
0	1	0
0,9889	0	-0,1018

Table 3: Thigh rotation matrix

-0,1115	-0,003	-0,9938
-0,0869	0,9962	0,0067
0,99	0,0871	-0,1113

Table 4: Shank rotation matrix

-0,1115	-0,003	-0,9938
-0,0869	0,9962	0,0067
0,99	0,0871	-0,1113

Table 5: Foot rotation matrix

Segment	LCS definition
Thigh	*Ot*: The origin coincident with KJC (knee joint centre). **KJC is defined in Table 4** **Yt**: The line connecting KJC and HJC, pointing proximally. **Xt**: The line perpendicular to the plane through HJC, LFE and MFE, pointing forward. **Zt: Xt^Yt**
Shank	*Os*: The origin coincident with AJC (ankle joint centre). **AJC is defined in Table 4** **Ys:** The line connecting AJC and KJC, pointing proximally. **Xs:** The line perpendicular to the plane through KJC, LM and MM, pointing forward. **Zs: Xs^Ys**
Foot	*Of*: The origin coincident with AJC (ankle joint centre). **AJC is defined in Table 4** **Xf**: The line coincident with **Xs** in the static posture. **Yf**: The line coincident with **Ys** in the static posture **Zf**: The line coincident with **Zs** in the static posture

Table 6: LCS definitions for leg segments

3.2. Numerical results

In this section all the numerical results are listed.

Numerical values of HJC, KJC, AJC's coordinates in global coordinate system are shown in table 7.

	Glob X	Glob Y	Globz
Glob HJC	-0,04	0,9051	0,3337
Glob KJC	-0,04	0,4351	0,3337
Glob AJC	-0,0389	0,0706	0,3018

Table 7: global coordinates of HJC, KJC, AJC

Numerical values of marker's coordinates in global coordinate system are shown in table 8.

	Glob X	Glob Y	Glob Z
Glob Rt	-0,0441	0,5597	0,4326
Glob LFE	-0,0951	0,4411	0,328
Glob MFE	0,015	0,429	0,3394
Glob Rs	-0,0582	0,1889	0,3405
Glob LM	-0,0754	0,0632	0,2804
Glob MM	-0,0025	0,0781	0,3233
Glob F1	-0,0475	0,0218	0,4286
Glob F2	-0,0781	0,0684	0,359
Glob F3	-0,1333	0,0232	0,3712

Table 8: global coordinates of matkers

Numerical values of relevant point's coordinates in local coordinate system for each segment are shown in table 9.

	Xt	Yt	Zt
Thigh_KJC	0	0	0
Thigh_HJC	0	0,47	0
Thigh_RT	0,0982	0,1247	-0,006
Thigh_LFE	0	0,006	0,055
Thigh_MFE	0	-0,006	-0,055

a)

	Xs	Ys	Zs
Shank_AJC	0	0	0
Shank_KJC	0	0,3658	0
Shank_Rs	0,0301	0,1213	0,0157
Shank_LM	-0,0165	-0,0091	0,0386
Shank_MM	0,0165	0,0091	-0,0386

b)

	Xf	Yf	Zf
Foot_AJC	0	0	0
Foot_F1	0,1307	-0,0376	-0,0059
Foot_F2	0,0611	0,0029	0,0325
Foot_F3	0,0833	-0,041	0,0858

c)

Table 9: value of coordinates of relevant points: a) Thigh LCS; b) Shank LCS; c) Foot LCS

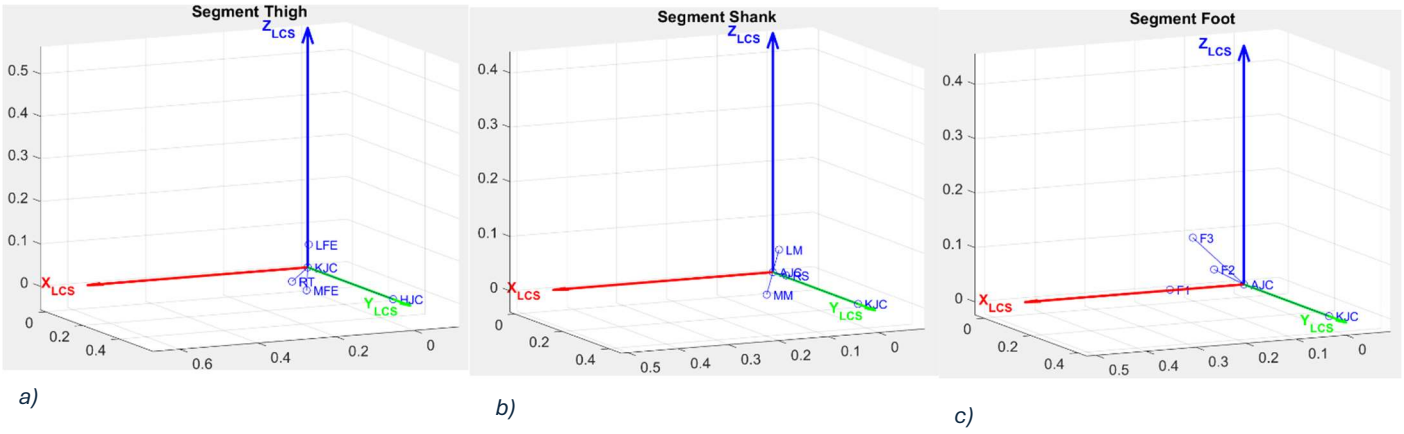

a) *b)* *c)*

Figure 4: LCS of the different segments: a) segment thigh; b) segment shank; c) segment foot

3.3. Leg model

LCS of the segments analyzed and rigid bar representing segments connecting HJC, KJC and AJC are shown in fig. 5. It's clearly possible to see that LCSs of shank and foot are coincident.

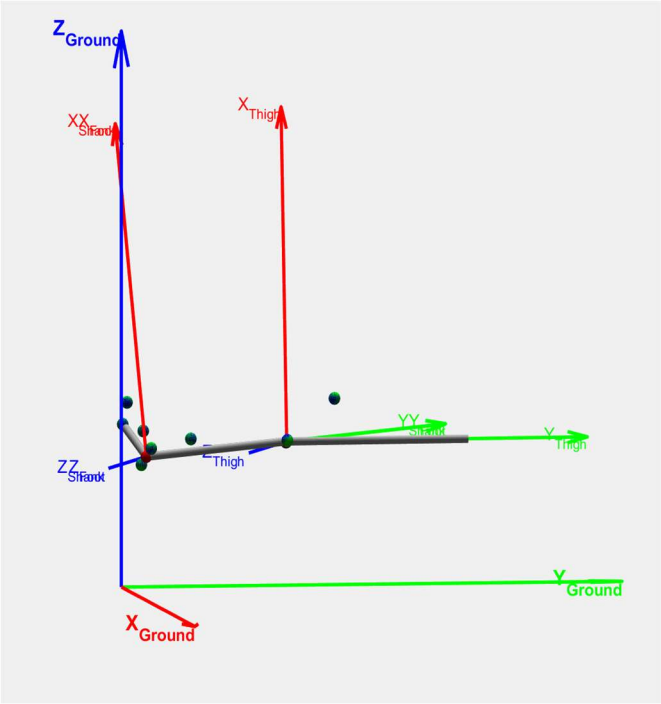

Figure 5: LCS of foot, shank, thigh

4. ANALYSIS OF RECONSTRUCTED MOTIONS

In the final stage of the project, an analysis of the 'reconstructed motion' and the temporal trajectories associated with all relevant angles was conducted, aiming to gain a detailed understanding of the reconstructed movement and the temporal dynamics of each studied parameter.

4.1. Flexion/Extension

Regarding knee flexion-extension, we can analyze the movement of both the knee and the ankle.

Specifically, for the knee, the graph shows three different lines, but only one of them highlights a movement. This is consistent with the fact that it is a revolute joint, which allows a single degree of freedom. The blue line represents the variation of the knee angle during the movement, accurately describing the flexion-extension. It is observed that the maximum angle reached is -114.868 degrees relative to the neutral axis, corresponding to the position of the fully extended leg.

To ensure the validity of the collected data, three authoritative scientific reference sites were consulted.

[3] [4] [5] The analysis of the information highlighted that the maximum knee flexion angle generally falls around 130 degrees. However, the value recorded during our study is slightly lower, suggesting that the patient involved in the experiment did not reach the theoretical maximum limit of knee flexion during the trial. This could be attributed to individual factors, such as potential physical limitations, joint stiffness, or other specific conditions of the subject examined.

Regarding the ankle, the graph illustrates its movement in relation to the knee's flexion-extension.

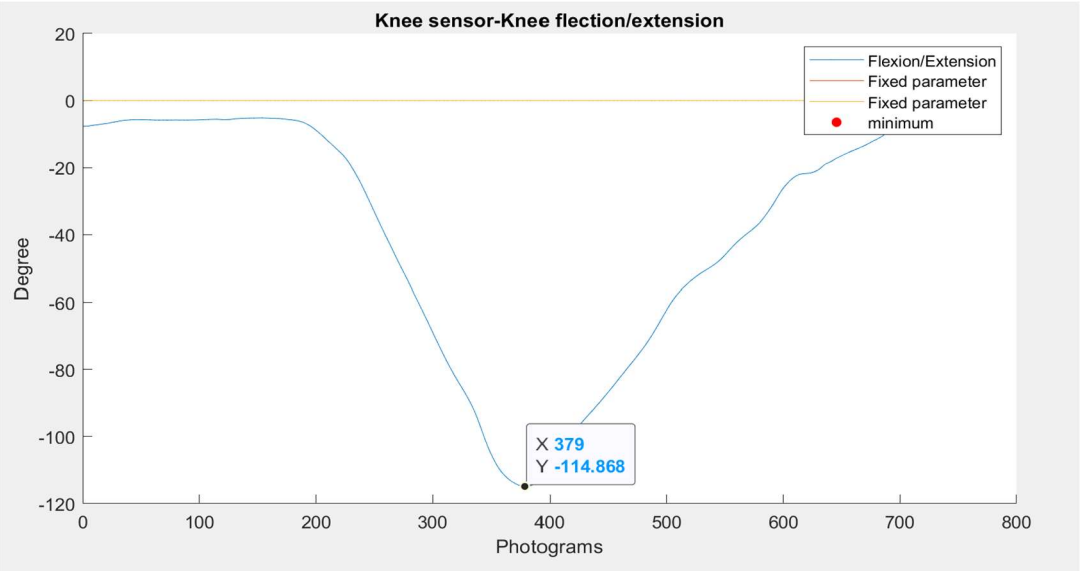

Figure 6: Knee sensor - Knee flection/extension

As a 'universal' joint, the ankle has two degrees of freedom, which explains why the graph shows one fixed line and two lines varying over time. One line represents dorsiflexion and plantarflexion of the ankle, while the other describes inversion and eversion movements. Similarly, these lines depict the changes in the ankle angles relative to the neutral axis.

Regarding dorsiflexion/plantarflexion, the maximum angle recorded is 19.9119 degrees, which approximately coincides with the point of maximum knee flexion, while the minimum angle is -0.718 degrees, a value that can be considered negligible. For the inversion/eversion component, the maximum angle reaches 7.38 degrees, while the minimum angle drops to -11.363 degrees.

These ankle movements, being related to the knee's flexion-extension, are less relevant from an analytical perspective. Therefore, although they vary over time and are interesting to observe, these ankle movements do not have a significant impact on the knee's behavior.

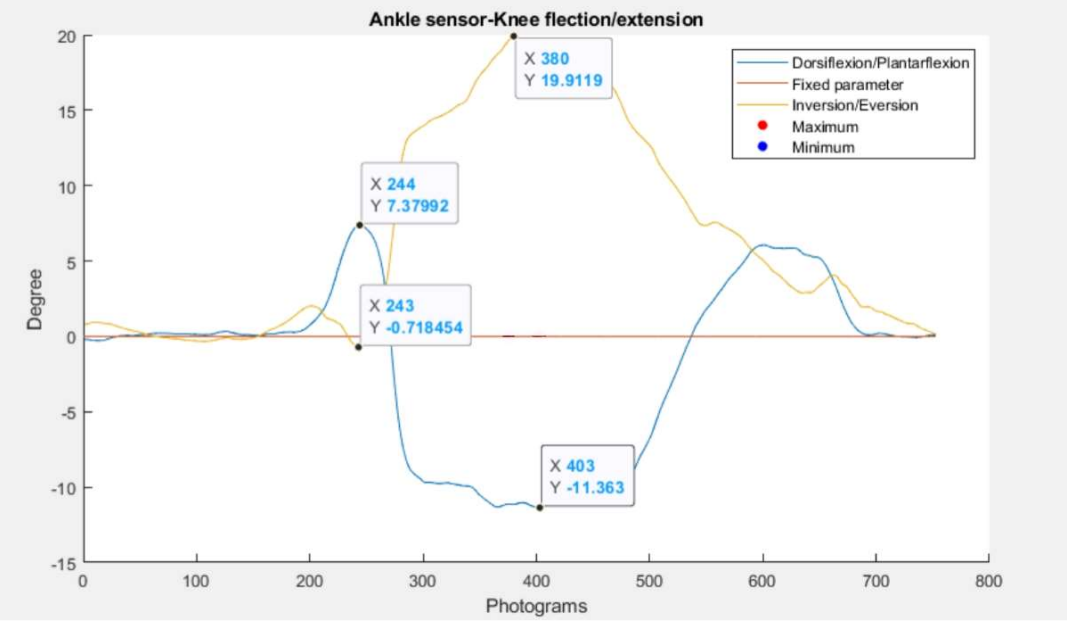

Figure 7: Ankle sensor - Knee flection/extension

4.2. Dorsiflexion/Plantarflexion

Regarding dorsiflexion and plantarflexion of the ankle, it is also possible to analyze the behaviour of both joints.

Regarding the knee, in this case, the graph also shows three distinct lines, but only one highlights a movement, as the joint has a single degree of freedom. Since the knee was kept suspended to allow the ankle to complete its full range of motion, the angle remained

constant at -105.338°. This result is fully consistent with the adopted experimental protocol.

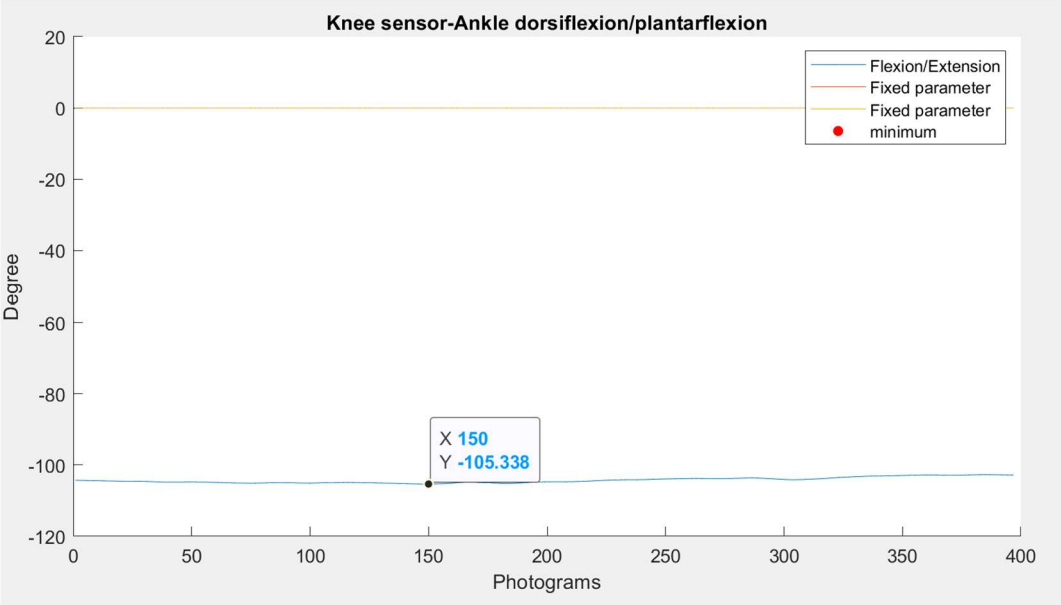

Figure 8: Knee sensor - Ankle dorsiflexion/plantarflexion

The ankle, being a joint with two degrees of freedom, allows two main types of movement: dorsiflexion and plantarflexion, which occur along the sagittal plane, and inversion and eversion, which develop along the frontal plane. The graph analyzes both of these movements through two main curves: the blue line represents dorsiflexion/plantarflexion, while the yellow line describes inversion and eversion, i.e., the lateral movements of the foot. Positive values on the Y-axis indicate dorsiflexion (movement of the foot upward), while negative values represent plantarflexion (movement of the foot downward).

The analyzed movement involved transitioning from full plantarflexion to full dorsiflexion and vice versa. The blue line shows significant variations over time, highlighting how the movement reaches a maximum dorsiflexion angle of 17.45° relative to the neutral axis and a minimum plantarflexion angle of -44.80°. [6] [7] These results are in line with the ranges commonly found in the literature, where dorsiflexion typically falls between 10° and 20° and plantarflexion between 30° and 50°.

The yellow line, on the other hand, remains close to zero for most of the movement, suggesting that inversion and eversion were limited or not significant compared to dorsiflexion and plantarflexion during the measured activity. This behavior could indicate that the lateral foot movements were either controlled or simply not relevant in the context being analyzed.

Finally, we can conclude that the collected data are consistent with the values documented in the scientific literature, making them useful for functional assessments or clinical comparisons.

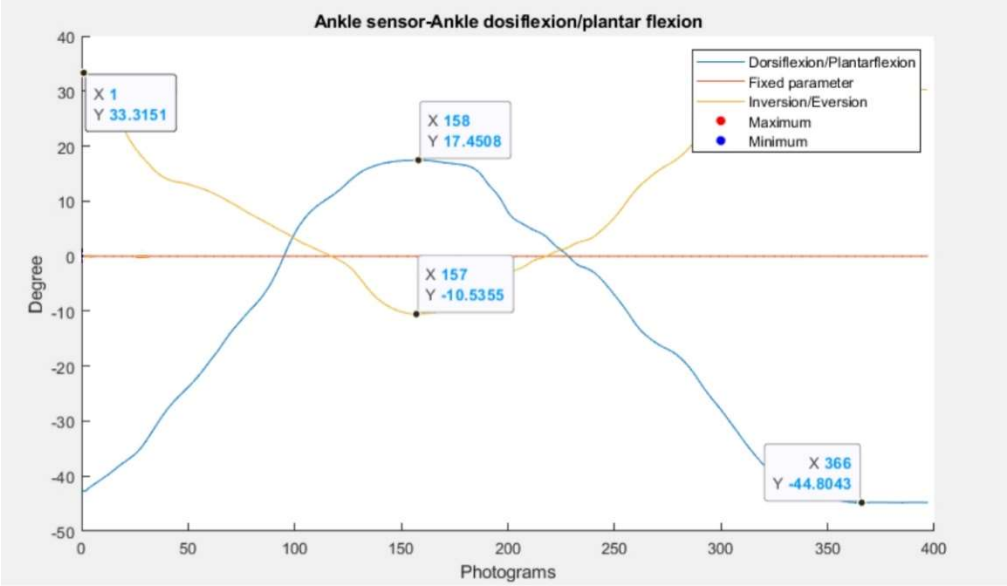

Figure 4: Akle sensor - Ankle dorsiflexion/plantarflexion

5. CONCLUSIONS

Human motion reconstruction is a highly significant technology with applications ranging from healthcare to robotics and improving sports performance. This work allowed a deeper understanding of the process of motion acquisition and analysis using the OptiTrack system, which is based on passive markers and synchronized cameras, demonstrating its ability to achieve an accurate three-dimensional representation of the movement of a right lower limb.

The main results include accurately identifying the leg model parameters, such as joint centers and local coordinate systems, and analyzing specific movements in detail, like knee flexion-extension and ankle dorsiflexion-plantarflexion. The system proved to be reliable, with a resolution of 1 mm, making it possible to reconstruct consistent and biomechanically relevant trajectories.

However, the experiment also highlighted some operational issues, such as the need for accurate camera calibration and precise marker placement. The interference between skin movement and underlying structures was a potential source of error, requiring careful attention during the preparation and execution of the experimental protocol.

A key aspect of this work was the opportunity to compare the obtained results with theoretical values and those reported in previous studies. For example, the maximum knee flexion angle, although slightly lower than the theoretical values, was still consistent with physiological limits and allowed for the consideration of possible individual or experimental factors. Additionally, the analysis of joint temporal trajectories provided valuable insights into the dynamics of movement and the behavior of the analyzed joints.

Looking ahead, it would be interesting to explore more complex applications, such as the analysis of multi-joint movements or interactions between the subject and robotic devices, as well as to integrate artificial intelligence systems to automate data analysis. Additionally, combining motion capture with complementary technologies, such as inertial sensors or advanced imaging systems, could further expand its capabilities, making it an increasingly comprehensive and versatile tool.

6. DISTRIBUTION OF WORK

The distribution of work has been equally divided between Alessandro Milazzo and Paolo Pagliaro (50% and 50%).

7. REFERENCES

[1] Nagymáté, G., & Kiss, R. M. (1970). Application of OptiTrack motion capture systems in human movement analysis. *Recent Innovations in Mechatronics*, *5*(1.). https://doi.org/10.17667/riim.2018.1/13

[2] *Calibration | EXTERNAL OptiTrack Documentation*. (n.d.). https://docs.optitrack.com/motive/calibration

[3] *The Ultimate knee Range of Motion chart*. (n.d.). https://www.kneepaincentersofamerica.com/blog/knee-range-of-motion-chart

[4] *Knee rehabilitation Exercises - OrthoInfo - AAOS*. (n.d.). https://orthoinfo.aaos.org/en/recovery/knee-conditioning-program/knee-pdf/

[5] Bunt, C. W., Jonas, C. E., & Chang, J. G. (2018, November 1). *Knee pain in adults and Adolescents: the initial evaluation*. AAFP. https://www.aafp.org/pubs/afp/issues/2018/1101/p576.html

[6] OrthoFixar. (2024, January 4). *Ankle range of motion*. OrthoFixar Orthopedic Surgery. https://orthofixar.com/special-test/ankle-range-of-motion/

[7] *Active Range of Motion (AROM) of the Ankle and Foot – Book Companion app*. (n.d.). https://book.physiotutors.com/content/ankle-and-foot-assessment/basic-assessment-of-the-ankle-and-foot/active-range-of-motion-arom-of-the-ankle-and-foot/